Measurement-Based Simulation of Lattice Gauge Theory Dynamics with Adaptive Quantum Circuits on a Trapped-Ion Processor

Takuya Okuda — University of Tokyo

Hiroki Sukeno — University of New Mexico
Enrico Rinaldi — Quantinuum

Talk at the University of Maryland | July 2026

Supported by JST Presto grant JPMJPR23F3

PRESTO
SAKIGAKE

Can measurements drive real-time gauge-theory dynamics?

Classical: sign problem

Euclidean Monte Carlo is powerful for equilibrium physics—but real-time transport, scattering, and nonequilibrium response require a different route.

Quantum: gauge constraint

Noise can drive the state outside the gauge-invariant sector, even while the hardware circuit continues to run.

Can measurements detect gauge constraint violations?

Measurement-based quantum simulation (MBQS)

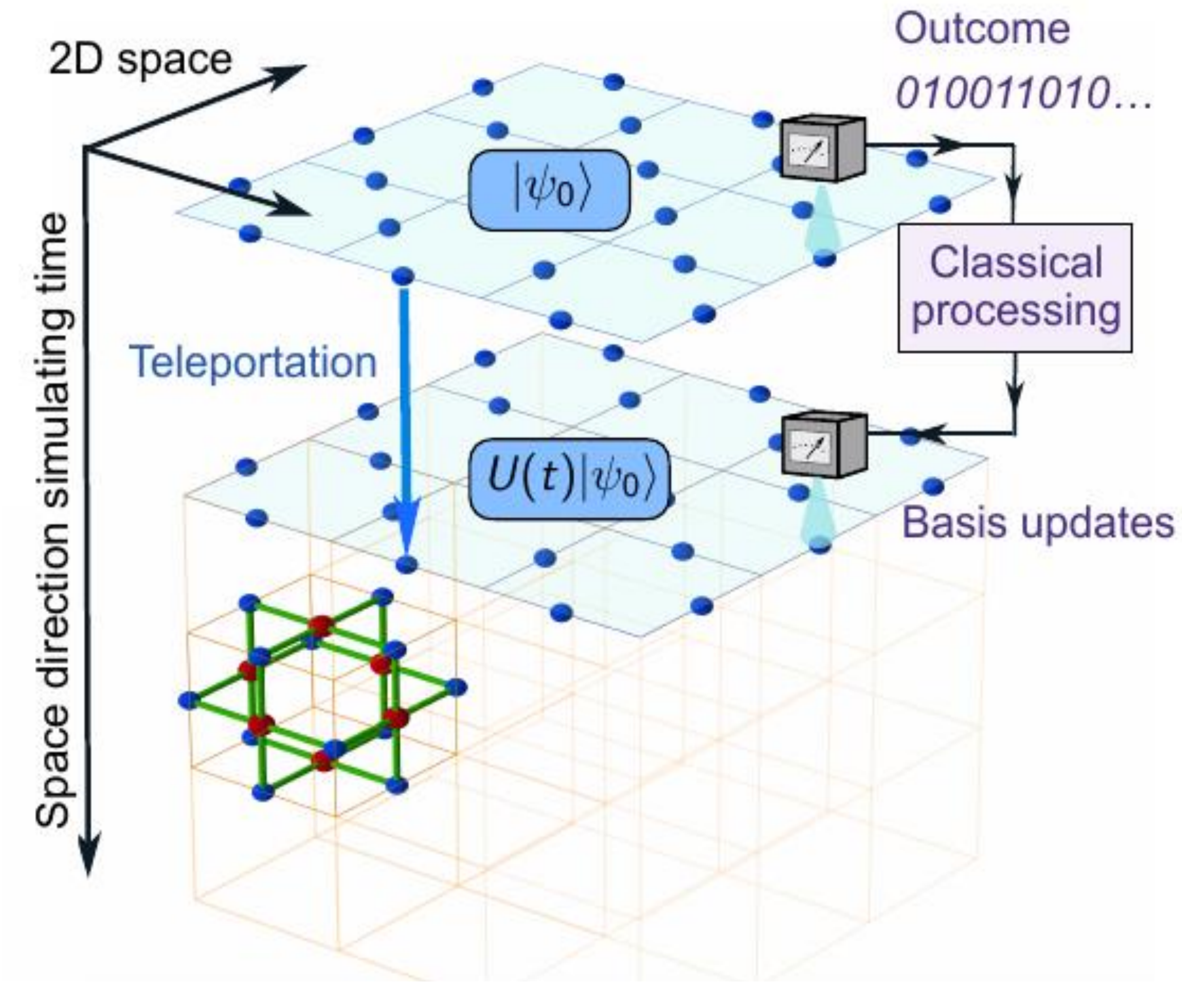

- Sukeno and I formulated MBQS in 2023.
- Special case of **measurement-based quantum computation (MBQC)**.

- Prepare an entangled **resource cluster state** designed for the target field theory.
- Measurements teleport the simulated state through successive layers.
- Classical processing tracks Pauli byproducts.
- Later measurement bases **adapt** to earlier outcomes.

The measurement record has two different roles

- Measurement outcomes drive time evolution and choose later measurement bases.
- Measurement outcomes also give resource-state symmetry syndromes.

Two information flows

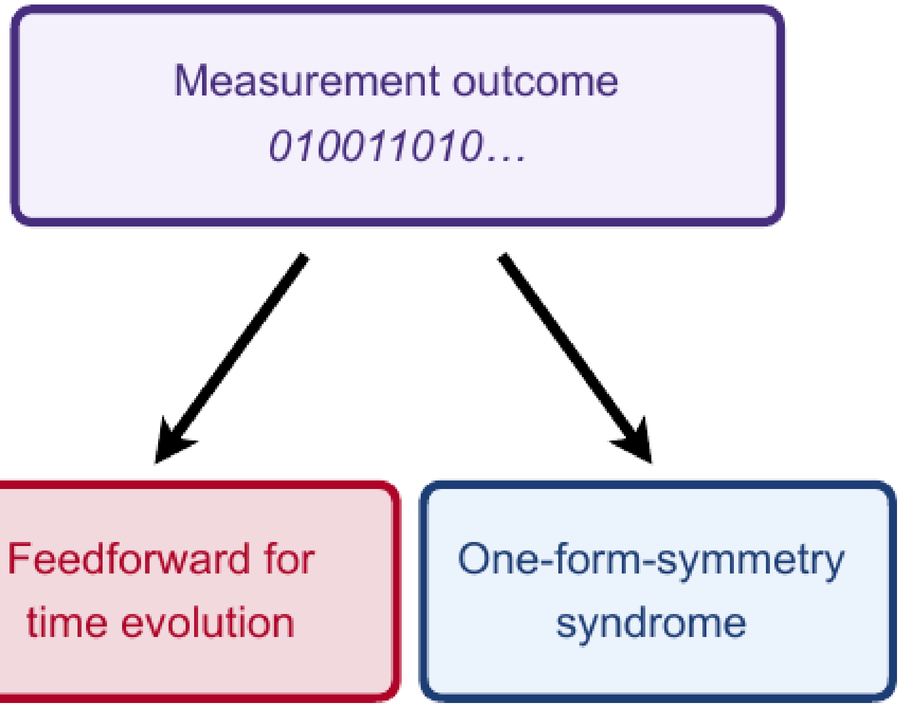

- Track byproduct operators
- Choose later bases

$$U(\mathcal{S}) = \prod_{e \supset v} X_e \qquad \begin{array}{ll} +1 & \text{keep} \\ -1 & \text{flag} \end{array}$$

Testbed: a (2+1)D Z_2 lattice gauge theory

$$H = -\sum_{\ell \in L} X_\ell - \lambda \sum_{p \in P} \prod_{\ell \subset p} Z_\ell$$

$$G(\mathbf{x}) = \prod_{\ell \supset \mathbf{x}} X_\ell = +1$$

- Qubits live on spatial links $\ell \in L$.
- Electric (X_ℓ) and magnetic terms ($\prod_{\ell \subset p} Z_\ell$) generate nontrivial (Trotterized) dynamics.
- Ideal evolution preserves the Gauss law constraint $G(\mathrm{x}) = 1$.

Experimental question

Can adaptive measurements generate this real-time evolution on hardware?

Quantinuum's H2 trapped ion processor with 56-qubit register

The same physical qubits are recycled

- Key capabilities: mid-circuit measurement, reset, and re-entanglement.
- All-to-all entangling connectivity.
- We generate an (instantaneous) resource state, consume it, regrow it by recycling qubits.

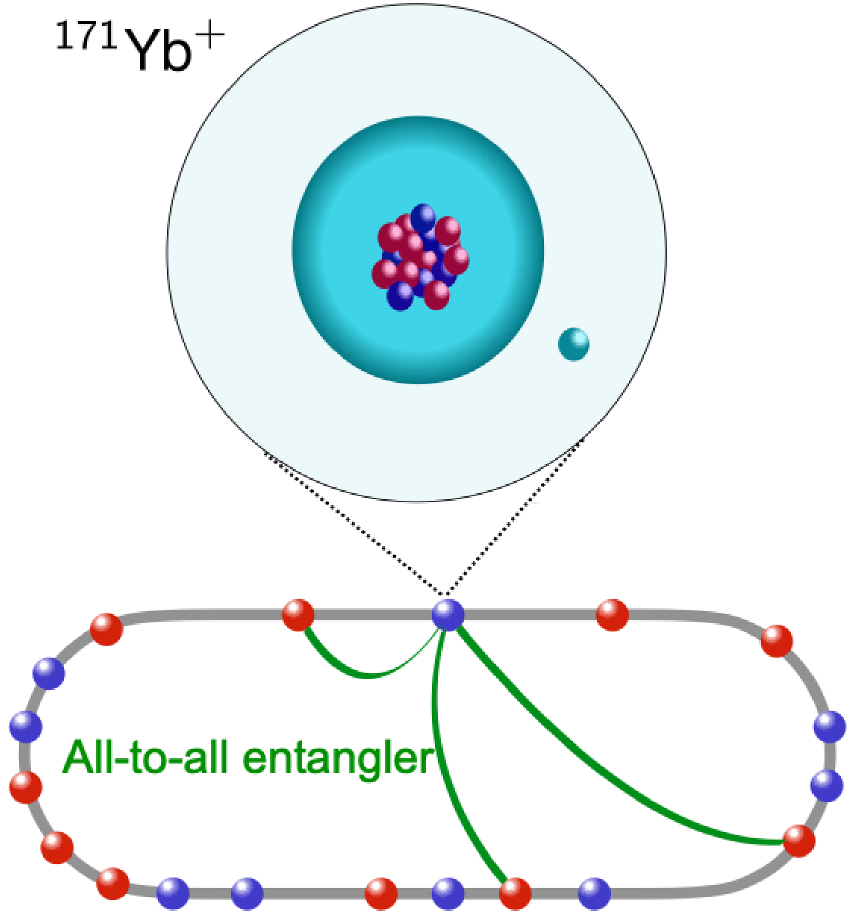

Qubit recycling enables a large virtual resource state

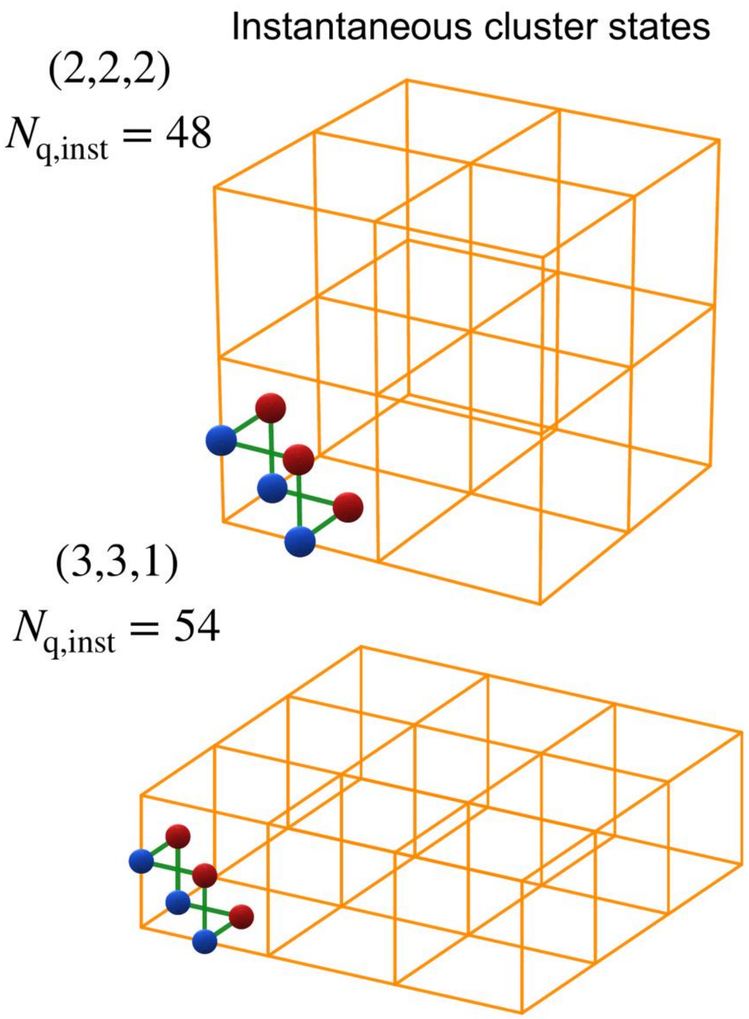

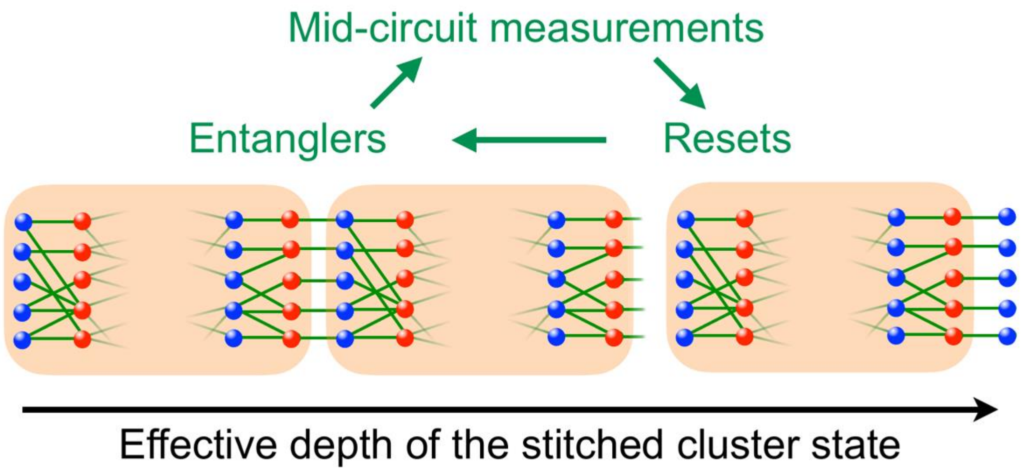

$2 \times 2 \times 14 \Leftrightarrow (2,2,2)$, 7 renewals
$3 \times 3 \times 8 \Leftrightarrow (3,3,1)$, 8 renewals

48 or 54 physical qubits are reused to realize a much larger spacetime resource state, e.g., 288-qubit virtual cluster state for coherent time evolution.

One-form symmetry makes resource errors visible

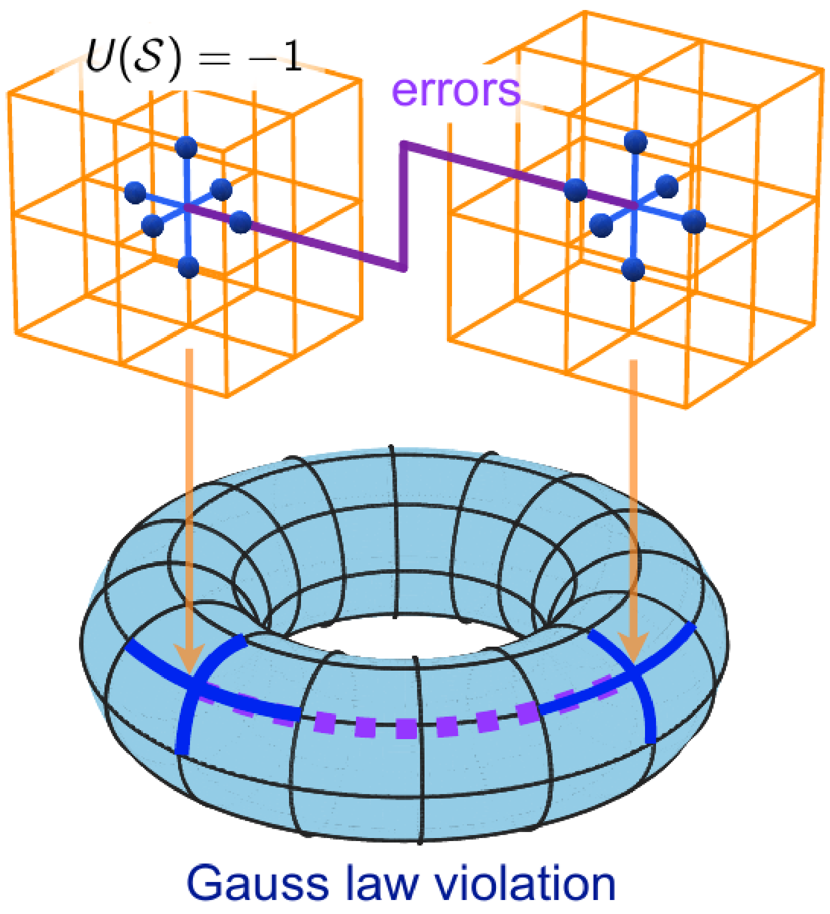

$$U(\mathcal{S}) = \prod_{e \in \mathcal{S}} X_e$$

- Ideal resource: $U(\mathcal{S}) = +1$ for every closed dual surface $\mathcal{S}$.
- A (-1)-outcome flags the existence of an error on the checked surface.
- Smallest surfaces are those surrounding resource-lattice vertices.

The resource syndrome is not itself a Gauss-law measurement

RESOURCE STATE

$$U(\mathcal{S}_v) = \prod_{e\in\mathcal{S}_v} X_e$$

Syndrome: computed from the X-basis outcomes on the edges.
A (-1)-value flags a detected resource-symmetry violation.

correlated under resource errors
→

SIMULATED 2D STATE

$$G(\mathbf{x}) = \prod_{\ell\supset\mathbf{x}} X_\ell$$

Measured independently at the output. Deviations from +1 diagnose Gauss-law violation.

Postselection keeps trajectories with no detected one-form-symmetry violation; undetected errors can remain.

Syndrome filtering stabilizes the Gauss-law diagnostic

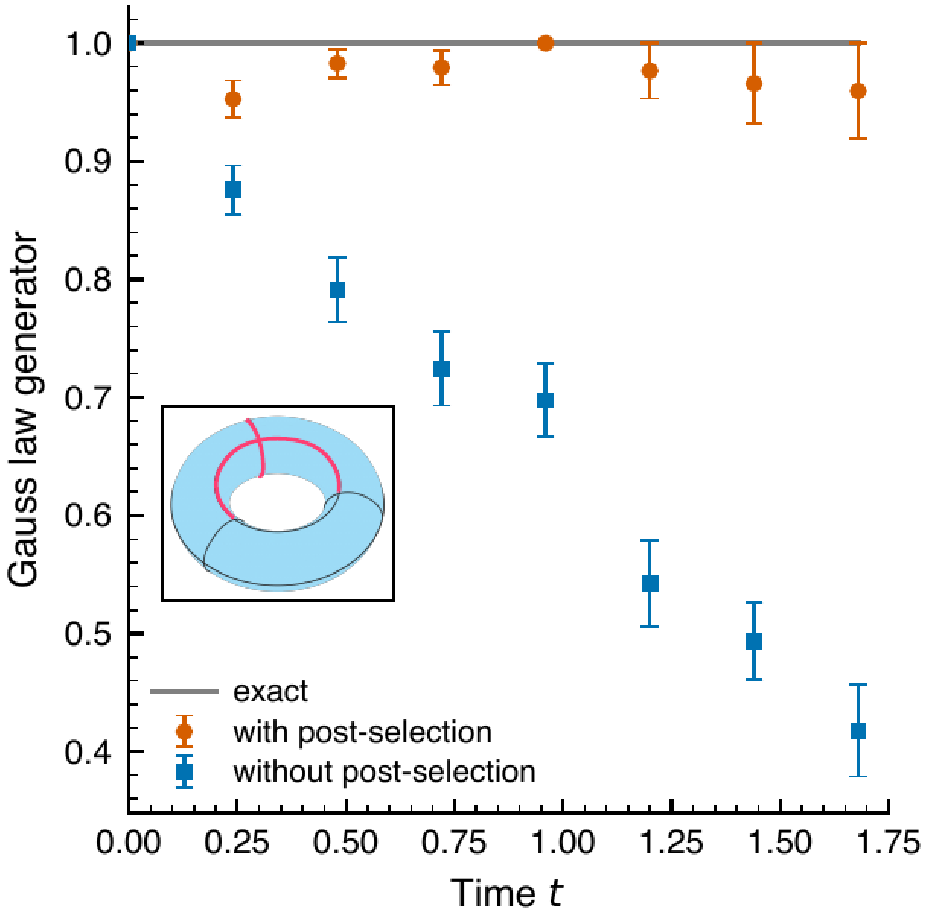

PRELIMINARY

After postselection, the Gauss law constraint is nearly satisfied.

- Orange: trajectories with no detected minimal-surface violation.
- Blue: all trajectories.
- 100 raw shots per time point; accepted counts decrease with depth.

Source: Figure 3b; finite-shot H2-2 data

Coherent dynamical evolution of plaquette operators

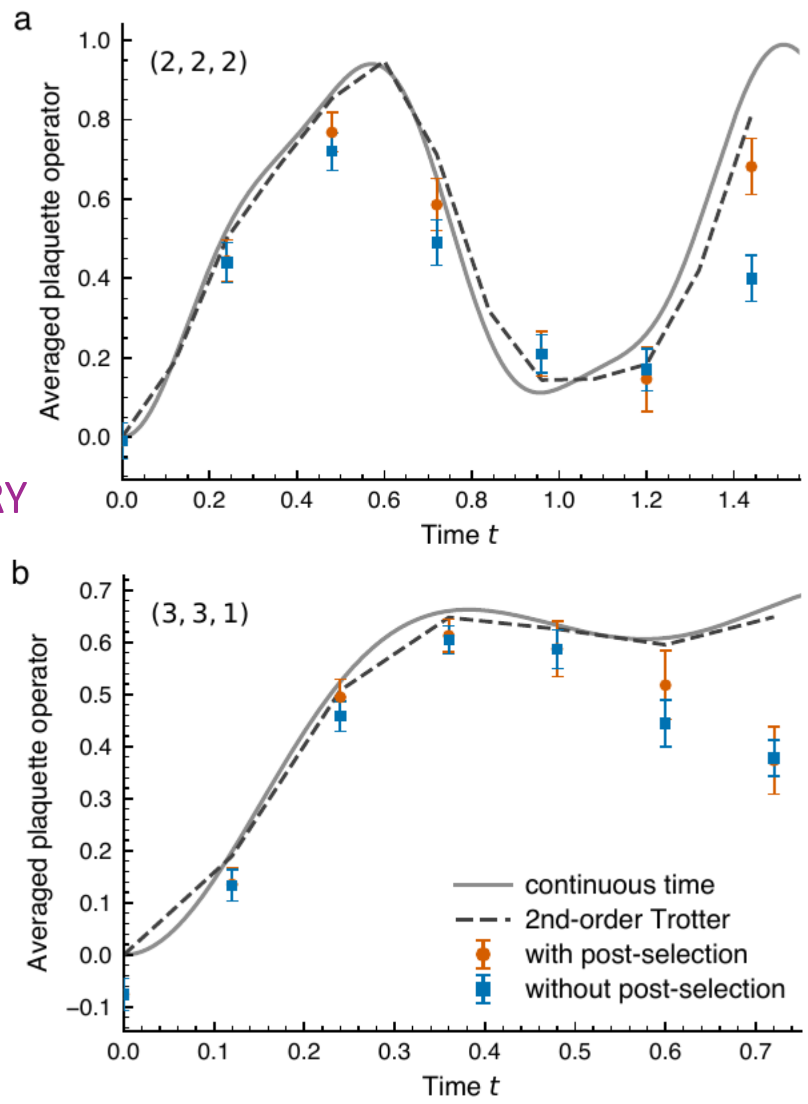

PRELIMINARY

2 × 2 x 2 instantaneous lattice: 296 virtual qubits and 576 entangling gates.

3 × 3 x 1 instantaneous lattice: 288 virtual qubits and 540 entangling gates.

Postselection improves aggregate agreement; late-depth deviations remain.

Qubit recycling realizes hundreds of virtual resource qubits

56

physical-qubit H2 register

288

virtual resource qubits in coherent dynamics

Virtual resource size counts cumulative number of qubits stitched through recycling—not simultaneously available physical qubits.

Postselection improves the retained data at a sampling cost

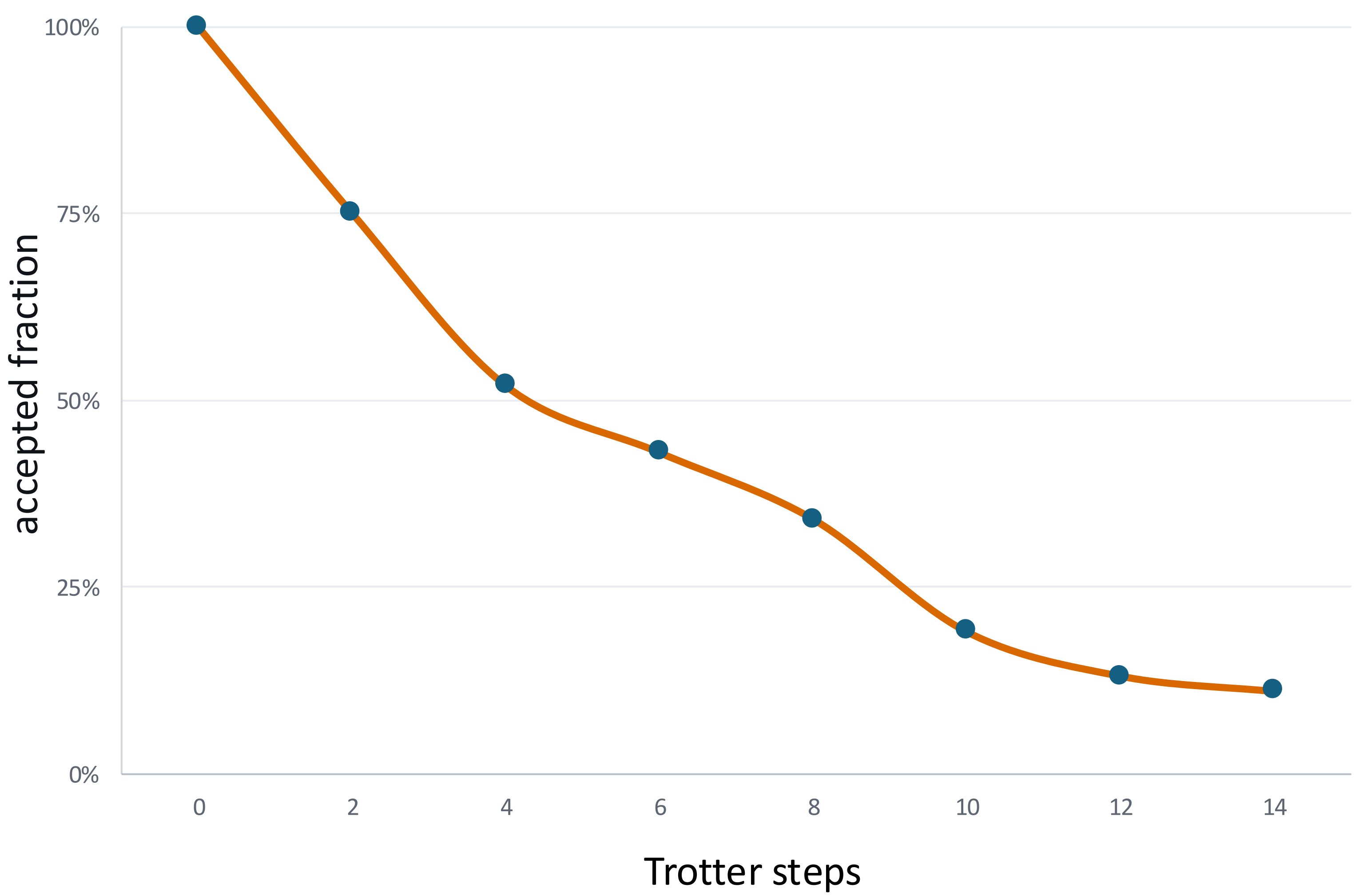

11 / 100

shots remain at the final plotted point for diagnostic

Rejection becomes costly as the checked spacetime volume grows.

What the experiment shows

1. Adaptive measurements drive real-time Z_2 gauge-theory dynamics on a trapped-ion device.

2. Qubit recycling realizes a virtual spacetime resource larger than the physical register.

3. The same measurement record drives the evolution and supplies symmetry syndromes.

Backup: stitched resource states retain high stabilizer values

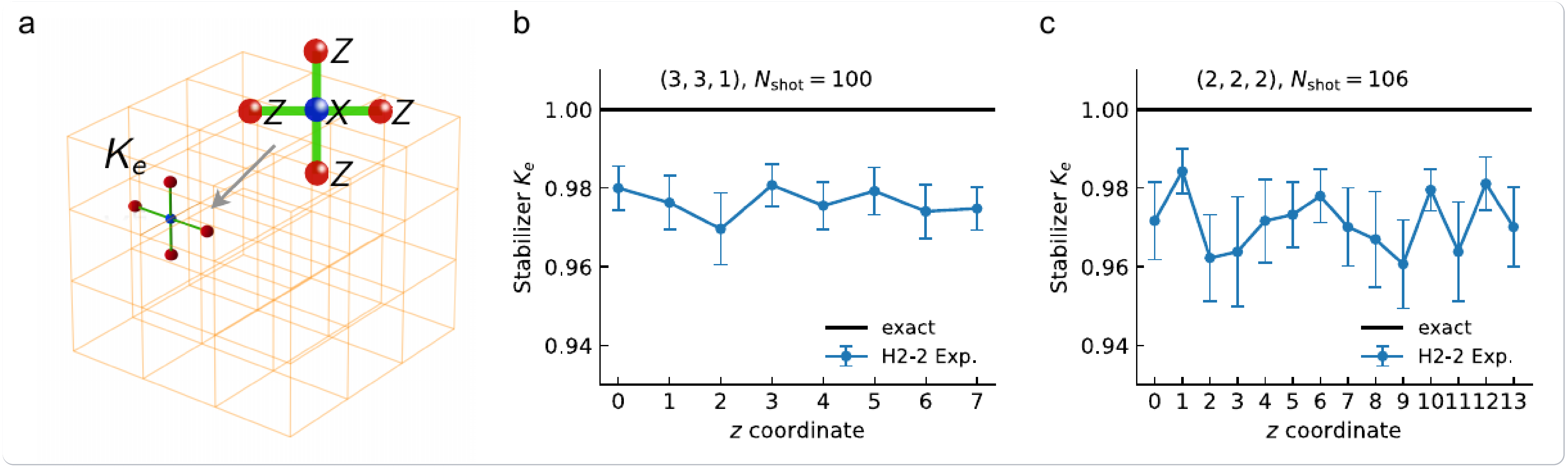

0.9763(28)

3 × 3 × 8 virtual resource
100 shots

0.9712(34)

2 × 2 × 14 virtual resource
106 shots

Source: Figure Ke and draft_arxiv.tex, lines 201–208; 100 and 106 shots

Nonlocal ’t Hooft-loop result

The syndrome contains information relevant to a gauge-invariant observable.

- The loop is measured independently at the output.
- Postselection improves aggregate agreement with exact Trotter evolution.
- This is error detection and rejection—not deterministic correction.

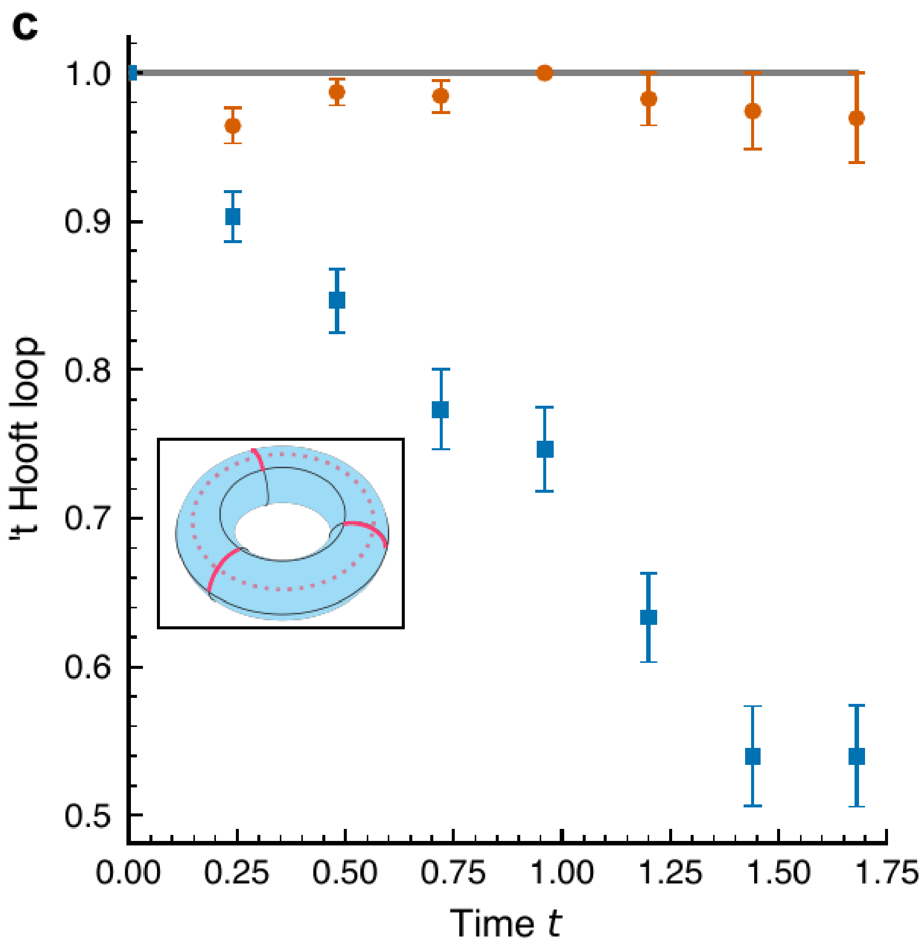

Source: Figure 3c; finite-shot H2-2 data

Backup: correction can replace rejection in principle

Detect endpoints

Nontrivial one-form syndromes mark open error-string endpoints.

Infer a recovery

A matching procedure proposes a recovery chain.

Update feedforward

Incorporate the recovery into the classical byproduct frame.

Next experimental step: make syndrome processing part of the adaptive control loop instead of discarding the shot.

Source: Sukeno–Okuda, SciPost Phys. 14, 129 (2023); not implemented on H2-2

Backup: 2 × 2 gate-based and MBQS comparison

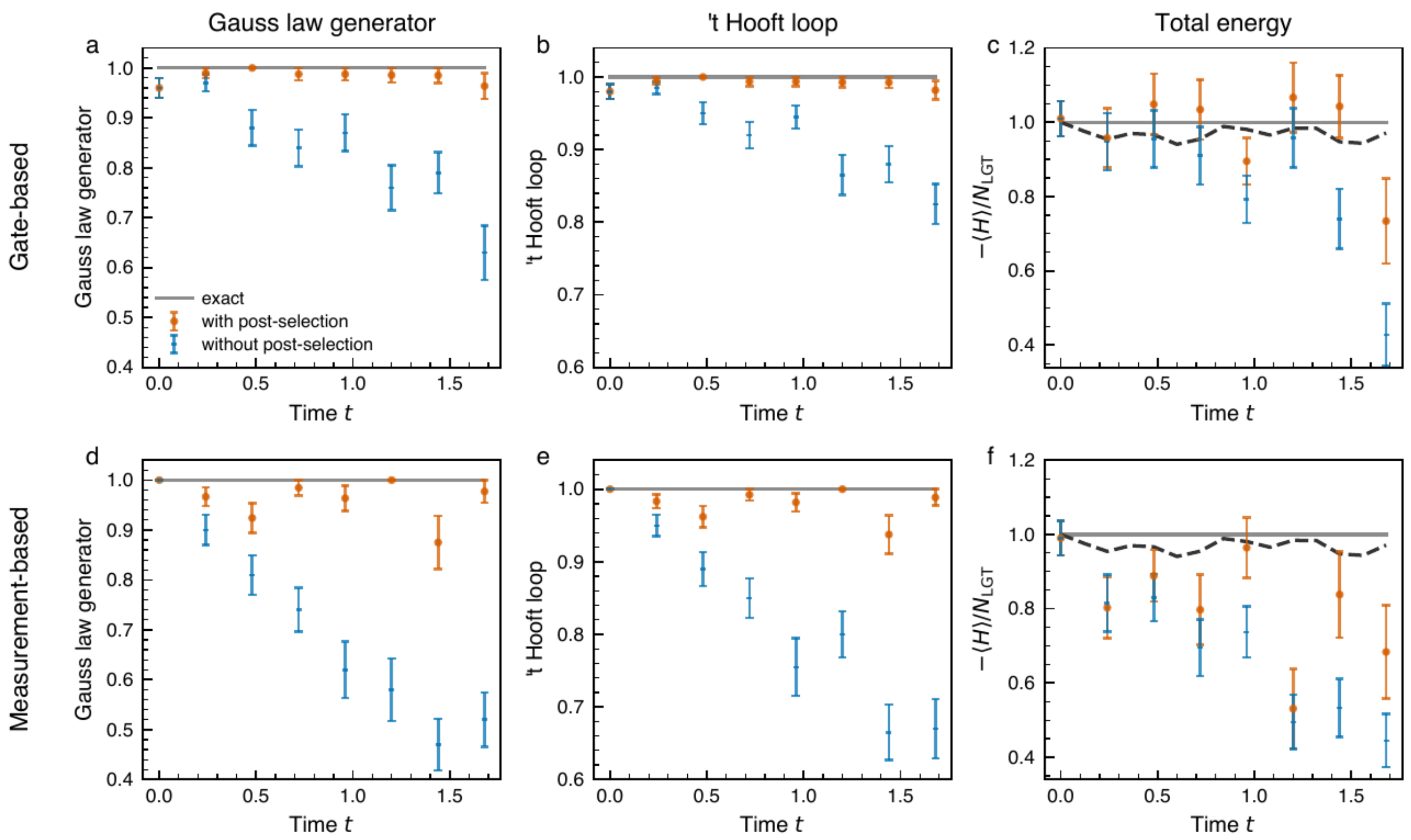

The gate-based circuit benchmarks the same target dynamics on the H2-2 processor.

Backup: 3 × 3 gate-based and MBQS comparison

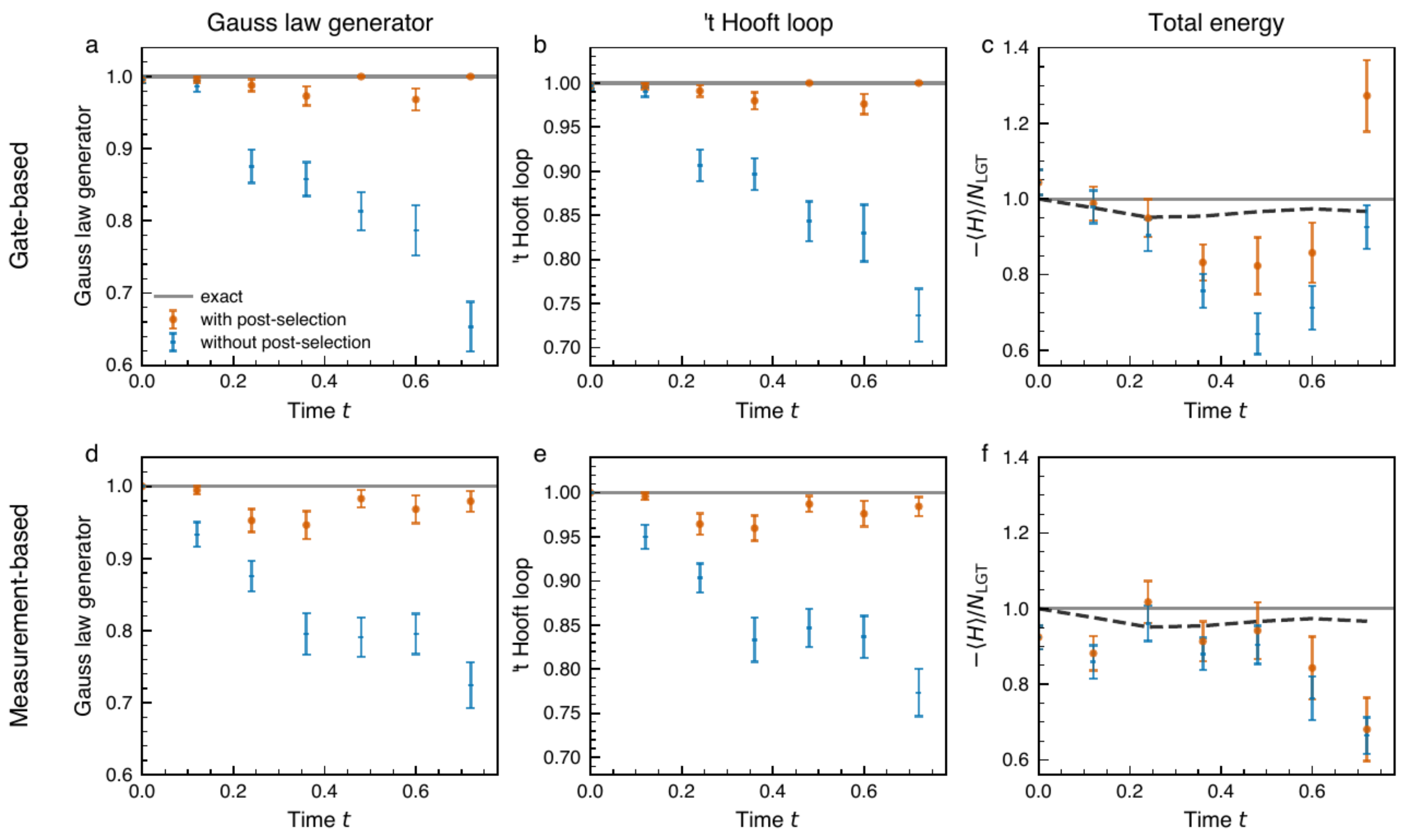

Both implementations target the same Trotterized dynamics; this is a benchmark.

Source: Figure GB-33; 100 shots per time point

Backup: measurement-driven simulation beyond Z_2

Z_n qudit gauge fields

Generalized cluster resources for finite cyclic groups.

Gauge fields with matter

Sparse model-specific connectivity can be retained.

Higher-form models

Wegner M(d,n) constructions provide a broader Abelian family.

Non-Abelian dynamics

A major open direction rather than a demonstrated extension.

Source: draft_arxiv.tex, lines 332–337; theory paper for established Abelian extensions